

RESEARCH ARTICLE SUMMARY

SPECIATION

Introgression dynamics of sex-linked chromosomal inversions shape the Malawi cichlid radiation

L. M. Blumer†, V. Burskaia†, I. Artiushin†, J. Saha†, et al.



Full article and list of author affiliations:
<https://doi.org/10.1126/science.adr9961>

INTRODUCTION: Ecological speciation is responsible for much of the biodiversity on our planet. Despite its fundamental importance, this process, in which new species emerge through evolutionary adaptation to distinct ecological niches, is still not fully understood. Intriguing case studies are adaptive radiations, bursts of ecological speciation that give rise to large numbers of diverse species over timescales that are short compared with the fixation time for new genetic variants. Genome sequencing studies increasingly point towards the importance of hybridization and cross-species gene flow in producing the diversity needed for ecological speciation and adaptive radiation. However, a major conundrum is the role of meiotic recombination in this process. On the one hand, recombination can create new, beneficial combinations of genetic alleles. On the other, it breaks down co-adapted allelic combinations, impeding speciation.

RATIONALE: Chromosomal inversions, stretches of DNA that are flipped in their orientation, provide a potential solution to the conflicting roles of recombination in ecological speciation. This is because inversions show suppressed recombination with the original chromosomal orientation, enabling them to lock together adaptive combinations of alleles in so-called “supergenes.” Inversions have been found to be important in ecological adaptation and speciation in many groups of organisms, but so far, there has been little evidence for their significance in adaptive radiations. To address this gap, we systematically investigated the presence and role of inversions across the lake Malawi cichlid fish adaptive radiation, the largest recent vertebrate radiation.

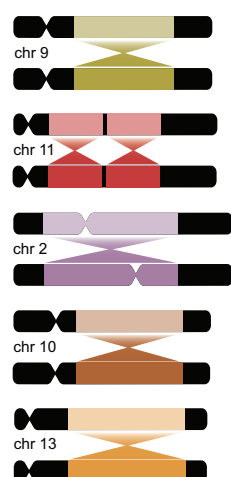
RESULTS: The genomes of 1375 Malawi cichlids from 240 species revealed the presence of multiple chromosomal inversions. The five largest of these segregate within the diverse and species-rich benthic subradiation, with a strong association between inversion states and habitat depth. Phylogenetic tracking of inversion states revealed a hybrid origin of the benthic clade, along with several introgression events transporting inversions and other genetic material between lineages within and outside of the radiation. Inversion haplotypes showed strong signals of adaptive evolution, including being enriched for sensory functions, behavior, and reproduction. For three chromosomes, the re-introgression of haplotypes of the ancestral orientation into benthic lineages coincides with an apparent Y chromosome-like role of this haplotype in the sex determination of some benthic species but not others.

CONCLUSION: The spread of chromosome-scale inversions in Malawi cichlids coincided with the phenotypic and ecological diversification of benthic species across habitats, with evidence for a role of inversion haplotypes in ecological adaptation. The additional transient sex linkage of introgressed inversion-region haplotypes points to an interplay of sex-linked and natural selection in shaping the evolution of inversion haplotypes and the diversification of cichlids. □

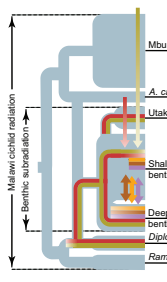
Corresponding author: H. Svardal (hannes.svardal@uantwerpen.be); R. Durbin (rd109@cam.ac.uk) †These authors contributed equally to this work. Cite this article as L. M. Blumer et al., *Science* 388, eadr9961 (2025). DOI: 10.1126/science.adr9961

Five large chromosomal inversions contribute to the diversification of Malawi cichlids. Inversions established in the diverse benthic subradiation. Inversion-region haplotypes were exchanged through hybridization of lineages within and outside of the Malawi radiation and contribute to ecological and habitat divergence, sensory adaptation, and sex determination.

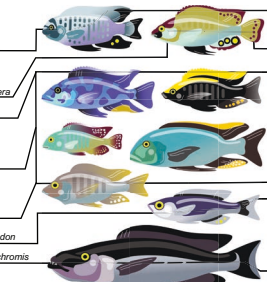
Five chromosome scale polymorphic inversions



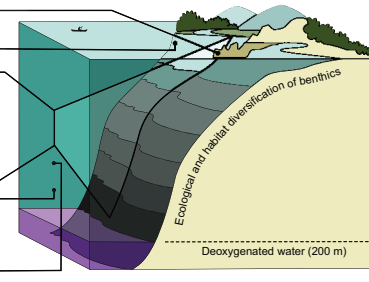
Inversions introgressed between lineages



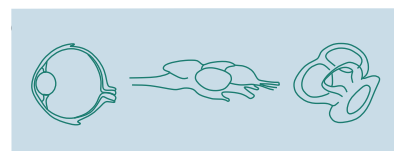
Shaped diversification of benthic clade



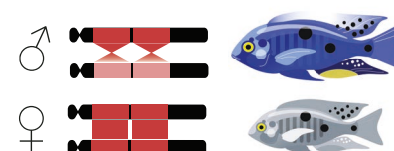
Involved in depth and substrate adaptation



Evolved under positive selection on sensory organs



Involved in sex determination



SPECIATION

Introgression dynamics of sex-linked chromosomal inversions shape the Malawi cichlid radiation

L. M. Blumer^{1†}, V. Burskaia^{2†}, I. Artiushin^{2†}, J. Saha^{2†}, J. Camacho Garcia², F. Campuzano Jiménez², A. Hooft van der Huysdinen², J. Elkin³, B. Fischer¹, N. Van Houtte², C. Zhou^{1,4}, S. Gresham², M. Malinsky⁵, T. Linderoth⁶, W. Sawasawa², G. Vernaz^{1,4†}, I. Bista^{7,8}, A. Hickey³, M. Kucka^{9§}, S. Louzada^{7¶}, R. Zatha¹⁰, F. Yang¹¹, B. Rusuwa¹⁰, M. E. Santos³, Y. F. Chan^{12,9}, D. A. Joyce¹³, A. Böhne¹⁴, E. A. Miska^{15,1}, M. Ngochera¹⁶, G. F. Turner¹⁷, R. Durbin^{1,4*}, H. Svartal^{2,18*}

Chromosomal inversions can contribute to adaptive speciation by linking coadapted alleles. By querying 1375 genomes of the species-rich Malawi cichlid fish radiation, we discovered five large inversions segregating in the benthic subradiation that each suppress recombination over more than half a chromosome. Two inversions were transferred from deepwater pelagic *Diplotaxodon* through admixture, whereas the others established early in the deep benthic clade. Introgression of haplotypes from lineages inside and outside the Malawi radiation coincided with bursts of species diversification. Inversions show evidence for transient sex linkage, and a notable excess of protein changing substitutions points toward selection on neurosensory, physiological, and reproductive genes. These results indicate that repeated interplay between depth adaptation and sex-specific selection on large inversions has been central to the evolution of this iconic system.

Understanding how biodiversity evolves is a fundamental question in biology. Whereas some evolutionary lineages remain virtually unchanged over hundreds of millions of years (1), others give rise to a great diversity of species over short evolutionary timescales (2). Adaptive radiations are particularly remarkable examples of explosive diversification, with many ecologically, morphologically, and behaviorally differentiated species emerging rapidly from a common ancestor. It is still not well understood how evolutionary lineages can produce such bursts of organismal diversity, but recent insights from genome sequencing point to a widespread contribution of “old” genetic variants (3), often introduced into populations by hybridization (4), and reused in new combinations that provide adaptation to novel ecological niches (5). A conundrum, however, is the role of meiotic recombination in this process. On one hand, recombination can create beneficial combinations of adaptive alleles (6). On the other hand, recombination can break adaptive combinations apart (7), especially in the face of

gene flow, producing unfit intermediates (8), and impeding speciation (9).

Chromosomal inversions, stretches of DNA that are flipped in their orientation, provide a mechanism to break the apparent deadlock between the beneficial and detrimental effects of recombination on species diversification by strongly suppressing recombination between the inverted haplotype and its ancestral configuration (7, 10, 11). Inverted haplotypes acting as “supergenes” can link together adaptive alleles that confer a fitness advantage in a specific environmental context or species background (12). In recent years, inversions have increasingly been found to contribute to adaptation (13, 14), genetic incompatibilities (15), assortative mating (16), sexual dimorphism (17, 18), mating systems (19), social organization (20), life-history strategies (21), and other complex phenotypes (11). Inversions are more common between sympatric than allopatric sister species in fruit flies (22), rodents (23), and passerine birds (24), pointing to their involvement in speciation with gene flow. However, despite their evolutionary relevance in other systems, there is relatively little information on their role in shaping large vertebrate adaptive radiations (25–28).

With more than 800 known extant species, Lake Malawi cichlids constitute the most species-rich recent vertebrate adaptive radiation (29, 30). The radiation was able to unfold and generate extraordinary morphological and ecological diversity despite repeated hybridization (31, 32) and conserved fertility across species (33). Previous studies found broad genetic association peaks for a behavioral phenotype important in assortative mating (34) in genomic regions that showed suppressed recombination in crosses of Malawi cichlid species (35). This raises the question of whether recombination-suppressing mechanisms, such as inversions, contributed to the adaptive diversification of Malawi cichlids.

In this work, we show that five large inversions segregate across and within many species and groups in the Lake Malawi radiation and systematically investigate their evolutionary histories and functions. By suppressing recombination, large chromosomal inversions can cause affected genomic regions to show evolutionary histories consistently distinct from the rest of the genome (36, 37). To detect regional deviations from the genome-wide evolutionary history, we obtained whole-genome sequencing (WGS) data from 1375 individuals of 240 Malawi cichlid species (table S1), detected 84 million single-nucleotide polymorphisms (SNPs), and first inferred genome-wide relationship patterns as a backbone (Fig. 1 and fig. S1) [see materials and methods; (38)]. Previous work suggested that the Malawi radiation evolved through serial diversification of three subradiations from a riverine-like ancestor (31): (i). A pelagic grouping of the mostly midwater *Rhamphochromis* and mostly deep-living *Diplotaxodon*; (ii) an ecologically and morphologically highly diverse benthic subradiation consisting of three subgroups, deep benthics, shallow benthics, and semi open-water utaka; and (iii) the predominantly rock-dwelling mbuna. The generalist-like stem lineage is represented today by the Malawi cichlid species *Astatotilapia calliptera* (which provided the reference genome for this study) (31, 39). Phylogenetic inference on our larger dataset confirms these major groupings and supports the branching order (Fig. 1).

¹Department of Genetics, University of Cambridge, Cambridge, UK. ²Evolutionary Ecology Group, Department of Biology, University of Antwerp, Antwerp, Belgium. ³Department of Zoology, University of Cambridge, Cambridge, UK. ⁴Wellcome Sanger Institute, Wellcome Genome Campus, Hinxton, UK. ⁵Institute of Ecology and Evolution, Department of Biology, University of Bern, Baltzerstrasse 6, Bern, Switzerland. ⁶W.K. Kellogg Biological Station, Michigan State University, Hickory Corners, MI, USA. ⁷Senckenberg Research Institute and Natural History Museum, Frankfurt am Main, Germany. ⁸LOEWE Centre for Translational Biodiversity Genomics, Frankfurt am Main, Germany. ⁹Friedrich Miescher Laboratory of the Max Planck Society, Max-Planck-Ring 9, Tübingen, Germany. ¹⁰School of Natural and Applied Sciences, University of Malawi, Zomba, Malawi. ¹¹School of Life Sciences and Medicine, Shandong University of Technology, Zibo, China. ¹²Groningen Institute for Evolutionary Life Sciences (GELIFES), University of Groningen, Nijenborgh 4, Groningen, Netherlands. ¹³Evolutionary and Ecological Genomics Group, School of Natural Sciences, University of Hull, Hull, UK. ¹⁴Leibniz Institute for the Analysis of Biodiversity Change, Museum Koenig Bonn, Adenauerallee 127, Bonn, Germany. ¹⁵Department of Biochemistry, University of Cambridge, Cambridge, UK. ¹⁶Department of Fisheries Headquarters, P.O. Box 593, Lilongwe, Malawi. ¹⁷School of Environmental and Natural Sciences, Bangor University, Bangor, Gwynedd, Wales, UK. ¹⁸Naturalis Biodiversity Center, Leiden, Netherlands. *Corresponding author. Email: hannes.svartal@uantwerpen.be (H.S.); rd109@cam.ac.uk (R.D.) †These authors contributed equally to this work. ‡Present address: Zoological Institute, University of Basel, Basel, Switzerland. §Present address: Department of Translational Genomics, University of Cologne, Cologne, Germany. ¶Present addresses: Laboratory of Cytogenomics and Animal Genomics, Department of Genetics and Biotechnology, University of Trás-os-Montes and Alto Douro, Vila Real, Portugal; BioSystems and Integrative Sciences Institute, Faculty of Sciences, University of Lisbon, Lisbon, Portugal.

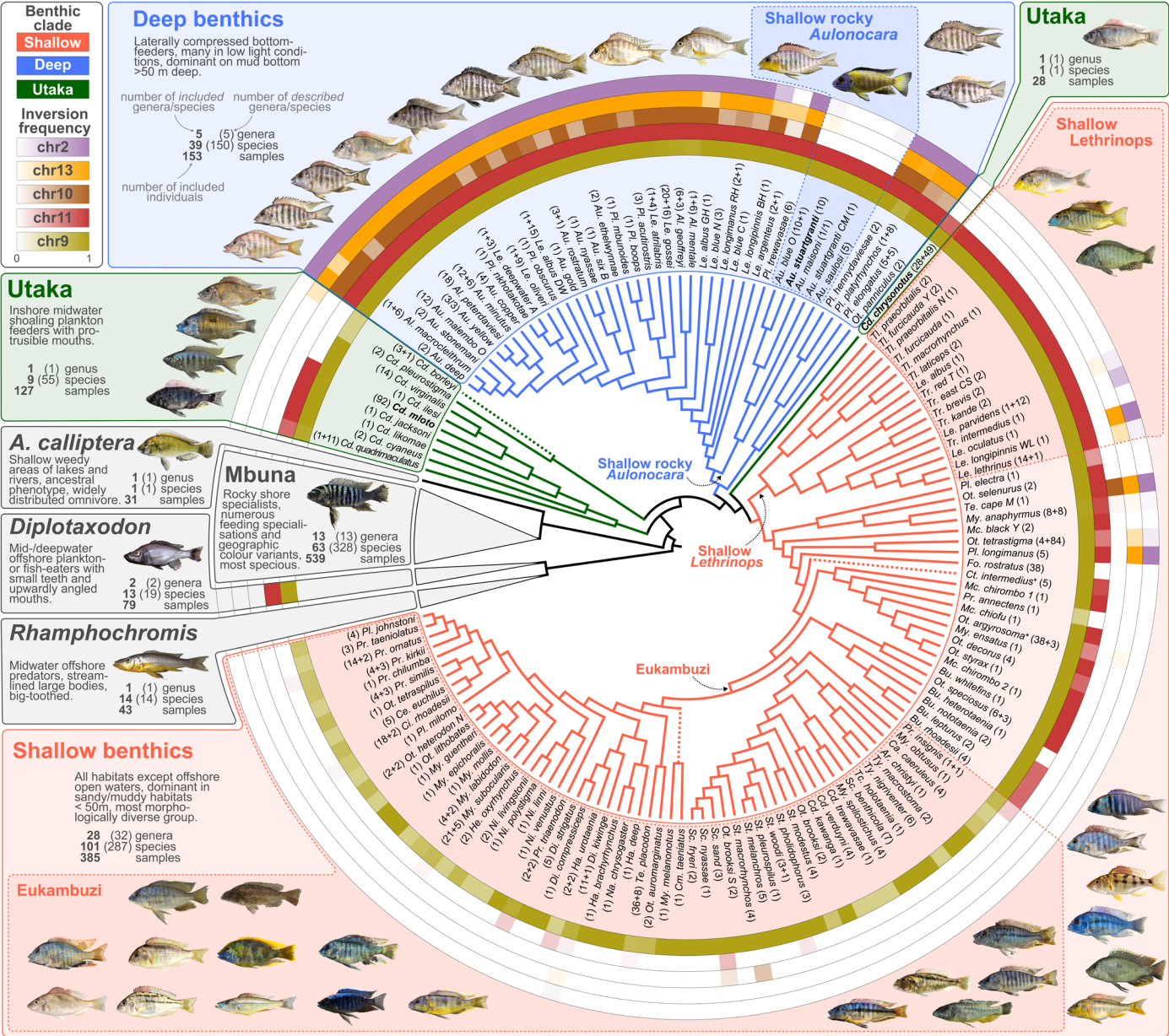


Fig. 1. Study system and prevalence of five large inversions. Consensus phylogeny of Malawi cichlid species used in this study (data S1) with inversion frequency based on WGS and PCR typing (38) shown in rings around the phylogeny (the same colors are used throughout the article). The benthic subradiation is expanded to show the phylogenetic position of each species and to highlight subclades that we refer to in the main text (shallow rocky *Aulonocara*, shallow *Lethrinops*, eukambuzi). Note that utaka are not monophyletic in this phylogeny. Nonbenthic groups of Malawi cichlids (i.e., the pelagic subradiations of *Rhamphochromis* and *Diplotaxodon*, the subradiation of predominantly rock-dwelling mbuna, and *A. calliptera*, a species distributed in rivers and margins around the lake that shares its putatively ancestral characteristics and genus assignment with riverine haplochromines outside of the radiation) are each represented by a single gray triangle approximately reflecting species richness relative to each other. Dashed lines indicate branches with unstable placement. See data S1 and S2 for full phylogenies with branch lengths and support values. Annotations next to species or clade names provide the numbers of sequenced and inversion-genotyped samples (additional samples that were inversion genotyped with PCR are indicated as + *n* in the annotation). Two taxa are annotated with a superscripted + to denote polyphyletic groups: *Otopharynx argyrosoma* contains a single *Cyrtocara moorii* individual, and *Ctenopharynx intermedius* contains two *Ctenopharynx pictus* individuals. Full species names are given in table S3, and inversion frequencies by species, in table S2. Species names for representative photographs are given in fig. S1. Tree files are given in data S1 and S2. Species subject to further experimental investigation are in bold.

Large inversions suppress recombination

We identified extensive genomic outlier regions consistent with polymorphic inversions on five chromosomes (2, 9, 10, 11, and 13), each spanning more than half a chromosome [between 17 and 23 mega-base pairs (Mbp)], using a clustering approach on our SNP data set (top panel, Fig. 2A, and figs. S2 and S3) (see materials and methods) (38).

A windowed principal component (PC) analysis (37, 40) of genetic variation revealed that these regions showed relationships among species of the diverse benthic clades of Malawi cichlids, which were very different from the rest of the genome (bottom panel, Fig. 2A, and fig. S4). Whereas, in the rest of the genome, PC1 tended to separate the three benthic subclades, in the focal regions, three distinct clusters

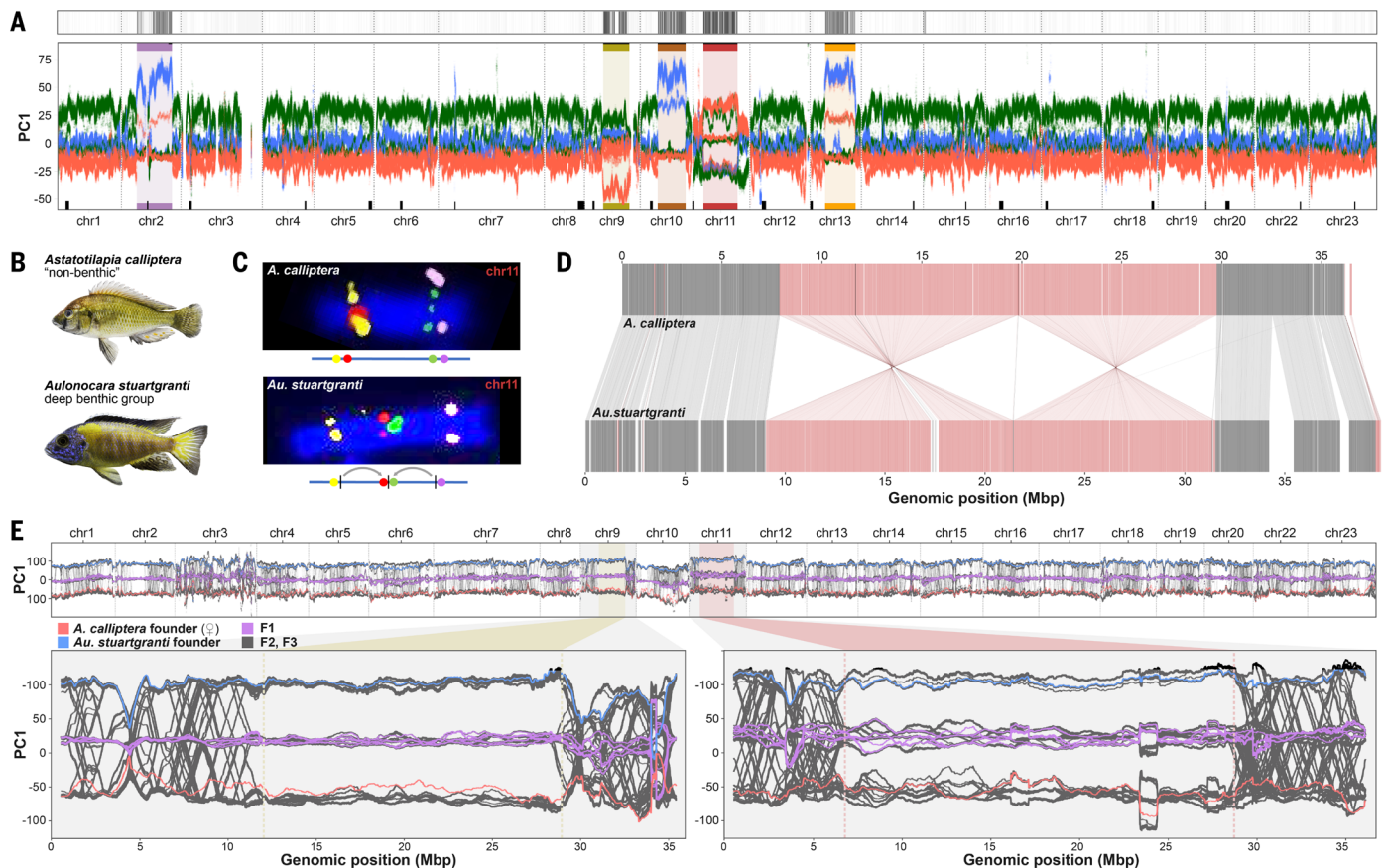


Fig. 2. Characterization of inversions. (A) (Top) Identification of genomic regions from clusters of aberrant phylogenetic patterns (38). (Bottom) First genetic principal component in overlapping 1-Mbp windows along chromosomes using the same colors for the benthic subclades as in Fig. 1. Outlier regions from the top panel are highlighted and color labeled. Centromeric satellite regions (for inference, see materials and methods; fig. S17; table S6; and text S1) (38) are indicated as black rectangles on top of the x axis. (B) Representative photographs of the species used in panels (C) and (D): *A. calliptera*, a lineage of the Malawi radiation distinct from benthics from which the reference genome was produced, and *Au. stuartgranti*, a species that genetically belongs to the deep benthic group but lives in shallow rocky habitats (clade shallow rocky *Aulonocara* in Fig. 1). According to WGS typing, the species are expected to show opposite orientations for the chromosome 9 and 11 inversions. (C) FISH of markers on chromosome 11 left and right of the putative inversion breakpoints show the expected noninverted orientation (top) in *A. calliptera*. In *Au. stuartgranti*, we see a double inversion (bottom; see fig. S8 for FISH of chromosome 9). (D) Whole-genome alignment of an ONT duplex long-read assembly of *Au. stuartgranti* to the *A. calliptera* reference assembly [which was rescaffolded with Hi-C data; see materials and methods (38)] confirms the double inversion on chromosome 11 (for other chromosomes, see fig. S9). (E) (Top) Windowed PC1 values of whole-genome-sequenced founders and progeny of an interspecific cross. Among 290 F2 and F3 individuals, no crossing-over events were observed in the inversion regions of chromosomes 9 (bottom left) and chromosome 11 (bottom right), whereas recombination was frequent in the flanking regions and on other chromosomes.

emerged that separated different groups of individuals and explained a much higher proportion of the genetic variance (fig. S5). Individuals in the intermediate cluster showed strongly increased heterozygosity, as expected for the heterozygous state of two divergent haplotypes (fig. S6). An exception to this was chromosome 9, where only two clusters (one with increased heterozygosity) emerged, consistent with the absence of one homozygous state. Overall, with double crossover events in only two deep benthic individuals, the clustering was consistent with nearly complete recombination suppression between inverted and noninverted haplotypes (fig. S7), as observed in other systems (22, 37, 41).

Using a combination of cytogenetics with long- and linked-read sequencing and de novo chromosome-level assembly of all five major clades of Malawi cichlids allowed us to confirm and characterize inversions in the regions on chromosomes 2, 9, 11, and 13 (but not chromosome 10 because of the lack of appropriate samples [see materials and methods; (38)] (Fig. 2, B and C, figs. S8 to S19, and table S4) and revealed additional smaller inversions that went undetected in the SNP analysis, including (i) a small inversion nested inside the large

inversion on chromosome 2, located next to the centromere (fig. S15 and text S1) (38), and (ii) two adjacent inversions on chromosome 20 (fig. S16 and text S1) (38).

To confirm the suppression of recombination between inverted and noninverted haplotypes, we performed an interspecific cross between *A. calliptera* and *Aulonocara stuartgranti* and whole-genome sequenced 290 individuals up to generation F3 (table S5). The absence of switching between the inversion-state clusters on chromosomes 9 and 11 on genomic PC1 axis in F2 and F3 individuals confirmed that recombination was fully suppressed in inversion regions of heterozygous F1s (Fig. 2E). Segregation ratios in F2s were Mendelian, except for the chromosome 11 inversion, which had a moderate deficiency of homozygotes for the *A. calliptera* haplotype (genotype proportions 20:66:43; χ^2 test on Mendelian ratios, $P = 0.016$).

Inversions segregate within benthic subradiation

Next, we investigated the distribution of inversion states across the phylogeny based on a multistep PC approach to infer inversion genotypes for all 1375 sequenced individuals ("WGS-typing") (Fig. 1, figs. S20

and fig. S21, and tables S7 and S8), denoting as noninverted or ancestral the orientation of the outgroup species *Pundamilia nyererei* (fig. S22) and *Oreochromis niloticus* (fig. S23). To further increase the number of genotyped individuals, we identified transposable element (TE) insertions highly correlated with inversion state and polymerase chain reaction (PCR)-typed insertions in an additional 401 individuals (fig. S24 and tables S9 to S11) [see materials and methods; (38)]. Together, these analyses revealed that all specimens of the mbuna and *Rhamphochromis* subradiations and *A. calliptera* were fixed for the noninverted, ancestral orientation for all five large inversions. All *Diplotaxodon* specimens also lacked the inversions on chromosomes 2, 10, and 13 but localized closer toward the cluster of inverted haplotypes than other nonbenthic clades in the PCA-based typing of the chromosome 9 and 11 inversions. In our de novo assembly for *D. limnothrissa*, both inversions are present (figs. S10 and S25), suggesting that *Diplotaxodon* are fixed for the inverted chromosome 9 and 11 haplotypes.

Among the benthic clades, the five inversions showed notably different frequencies across the species: for chromosomes 2, 10, and 13, the inverted state was fixed or at high frequency in most deep benthic species but almost absent among shallow benthic species and utaka. For chromosomes 9 and 11, the inverted states were fixed in most benthics, with the major exception of a large monophyletic subclade of shallow benthics in which chromosome 11 was mostly fixed for the ancestral noninverted state and in which chromosome 9 was mostly polymorphic. We will refer to this group as “eukambuzi,” inspired by the local name “Kambuzi” for some members of this group (Fig. 1). The distribution of inversion frequencies was consistent with a scenario in which inversions on chromosomes 2, 10, and 13 rose to high frequencies in an ancestor of the deep benthic lineage, whereas the inversions on chromosomes 9 and 11 rose to high frequency in the ancestors of two nonsister groups, pelagic *Diplotaxodon* and benthics, but with one monophyletic subgroup of the benthics (eukambuzi) retaining or regaining the noninverted ancestral state.

Origins and introgression patterns of the inversions

To better understand the evolutionary histories in inversion regions, we estimated genetic divergence times between Malawi cichlid species for the five inversion regions (both the inverted and noninverted haplotypes) and the remaining noninverted regions of the genome (Fig. 3A and fig. S26). We found that, outside the inversions, benthics were least divergent from *Diplotaxodon* and *A. calliptera* (Fig. 3A, top row), a pattern that is inconsistent with the inferred phylogenetic position of benthics as a sister group to mbuna and *A. calliptera* [e.g., (31), Fig. 1, and data S2] but rather suggests that benthics arose through admixture between the *Diplotaxodon* and *A. calliptera* lineages after their respective splits from *Rhamphochromis* and mbuna (Fig. 3B; see text S2 for more detailed discussion). Such a hybrid benthic origin model also provides a parsimonious explanation for the sharing of the chromosome 9, 11, and 20 inversions between all *Diplotaxodon* and most benthics (indicated by ④, Fig. 3B; figs. S9 to S12) and explains the general strong affinity of all inverted haplotypes to *Diplotaxodon* (Fig. 3A, right).

The origins of noninverted benthic haplotypes appear to be more diverse. The noninverted benthic chromosome 11 haplotype is closest to *A. calliptera* (Fig. 3A, row 3), as expected if this haplotype was contributed from *A. calliptera* in the original founding of benthics. However, previously inferred signals of gene flow between shallow benthics and *A. calliptera* relative to deep benthics (31) and the relatively low heterozygosity of this haplotype (fig. S27), which is mostly present among eukambuzi, could alternatively point to its later introgression from *A. calliptera* (event ③, Fig. 3B).

For chromosome 9, benthics are almost fixed for the inversion with only some individuals, mainly eukambuzi, being heterozygous. However, it is notable that the noninverted haplotype found in benthics is much more divergent from the rest of the Malawi radiation than any

other inversion haplotype and the rest of the benthic genome (row 2, Fig. 3A). To follow this up, we produced a second SNP callset including a wide variety of related African cichlid species (“haplochromines”) and computed ABBA-BABA tests (32, 42) (text S2, fig. S28, and tables S12 and S13) (38). This revealed strong excess allele sharing of the noninverted benthic chromosome 9 haplotype with *Pseudocrenilabrus philander*, one of the few outgroup species present today in the catchment of Lake Malawi ($D = 0.45$; block-jackknifing z -score = 6.5; family-wise error rate-corrected $P = 4 \times 10^{-9}$). We concluded from this that the chromosome 9 noninverted benthic haplotype is not closely related to other Malawi haplotypes but instead arrived in an ancestor of eukambuzi through admixture with a lineage containing *Pseudocrenilabrus*-like genetic material (⑥, Fig. 3B).

The remaining inversions on chromosomes 2, 10, and 13 are all common among deep benthics and rare or absent among shallow benthics and utaka, suggesting that they rose to high frequency early in the deep benthic lineage (Fig. 3B). This is also consistent with the phylogenetic relationships within the inversion regions (figs. S29 to S33), which suggest that the few cases of deep benthics with noninverted states and shallow benthics with inverted states are due to a limited number of later gene flow events, the most consequential of which are indicated in events ⑤ to ⑥ in Fig. 3B (see text S2 and fig. S34 for a more comprehensive analysis). Most of these events transmitted more than one inversion haplotype as well as genetic material outside the inversion regions (Fig. 3C) (42).

Although there is evidence for each of the admixture and introgression events described in Fig. 3B and fig. S34, other more complex scenarios are also possible. Furthermore, additional minor introgression events and/or incomplete lineage sorting (ILS) are required to explain the final patterns of occurrence of the inversions. However, the alternative hypothesis of random segregation through ILS giving rise to the observed patterns is not supported. First, inference based on coalescent calculations yields a probability of only 0.02% for retaining shared polymorphism among deep and shallow benthics at three inversions through ILS [(28); see materials and methods (38)]. Second, an ABBA-BABA analysis confirmed that signatures of introgression outside of inversions were much more common when deep and shallow benthic species shared their inversion state compared with cases where they differed in inversion state (Fig. 3C), a pattern that is not expected under ILS.

Inversion divergence between deep- and shallow-living lineages

All five inverted states are found at higher frequencies in deepwater-living species (fig. S35 and table S14). The corresponding regions show increased relative divergence and reduced cross-coalescence rates (a measure of genetic exchange) compared with the rest of the genome and, for chromosomes 2, 10 and 13, also disproportionately high effect sizes in a population structure-corrected genome-wide association study between deep and shallow benthics (Fig. 3A and figs. S36 to S40) [see materials and methods; (38)]. Further, the inversion transmission events inferred above (Fig. 3B and fig. S34) were often such that species living at depths atypical for their clade (e.g., shallow-living rocky *Aulonocara* of the deep benthic clade and deep-living shallow benthic species, such as *Trematocranus* sp. “Cape Maclear”) had received the inversion haplotypes of species living at similar depths (fig. S35). Together, these observations support the hypothesis that inversion haplotypes contributed to divergence along a depth gradient.

Pervasive signatures of adaptation on inversion haplotypes

Next, we investigated whether the evolution of inversion haplotypes was driven by adaptive processes and could potentially constitute “supergenes” of coadapted alleles. To identify genetic variants relevant for the early evolution of inversion haplotypes, we computed correlation coefficients and significance scores ($-\log_{10}P$) between SNP and inversion genotypes (figs. S41 and S42), where positive correlation coefficients correspond to derived SNP alleles on inverted haplotypes

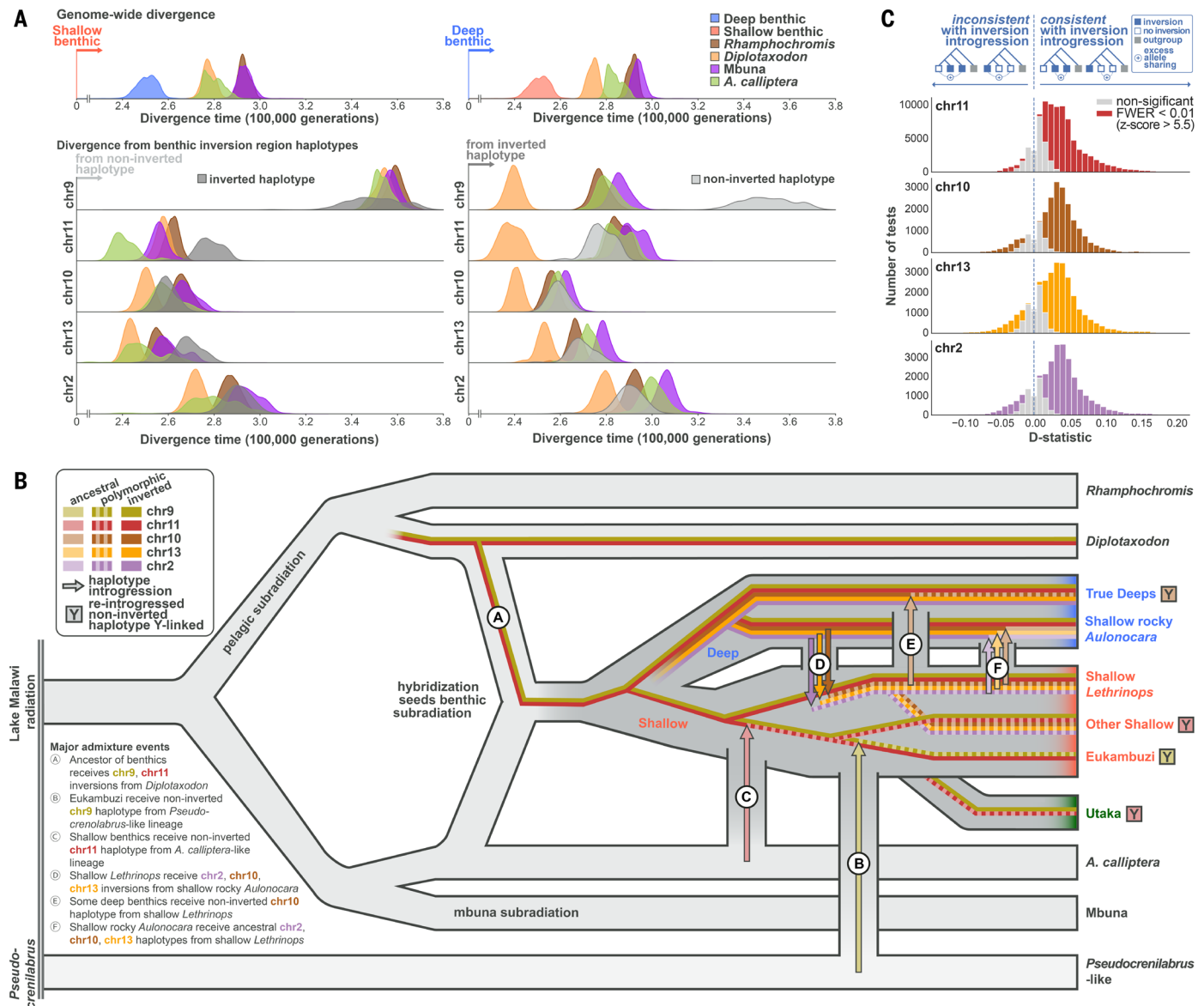


Fig. 3. Evolutionary history scenario of inversion haplotypes. (A) Density plots of pairwise sequence divergence translated into divergence (coalescence) times assuming a mutation rate of 3×10^{-9} bp per generation (31). The top panels show results for the genome outside the five large inversions, comparing all major clades against shallow benthics (left) and deep benthics (right). Panels below the top row show divergence in inversion regions for the noninverted (left) and inverted (right) benthic haplotypes. (B) A simplified model for the evolutionary history of the Malawi cichlid radiation, which includes several inversion haplotype transmission events. Vertical gray connections indicate major gene flow events. Letter-labeled arrows indicate transfer of inversion-region haplotypes. For further events, see fig. S34. Lineages in which re-introgressed inversion region haplotypes of ancestral orientation apparently play a Y-like role in sex determination (see Fig. 5 and main text) are indicated by Y. (C) Evidence for transfer of inversion haplotypes through introgressive hybridization. Histograms of ABBA-BABA statistics $D(P1, P2, P3, Outgroup)$ calculated outside the inversions. For the different panels, we selected those ABBA-BABA tests for which the inverted state of the respective chromosome is present in one of the two more closely related species P1 and P2 but absent in the other and ordered them such that P2 shared the inversion state (presence or absence) with P3. In such a configuration, significantly positive values are suggestive of gene flow outside of inversions between the species sharing inversion states, whereas significantly negative values suggest gene flow between species not sharing inversion states. Under the null hypothesis of no inversion introgression, the statistic would be symmetric around zero. FWER, family-wise error rate.

and negative coefficients to derived SNP alleles on noninverted haplotypes. We expected the most highly inversion correlated SNPs (ICS) to contain variants relevant in early inversion evolution.

ICS were much more likely to be in protein coding regions compared with other SNPs on all five chromosomes (Fig. 4A) and showed a strong excess of nonsynonymous divergence in McDonald-Kreitman-type tests (fig. S43), indicating that positive and/or relaxed purifying selection contributed to inversion haplotype divergence. To confirm that there was a component of positive selection and not just drift due to

relaxed purifying selection, as expected when a single haplotype rapidly raises in frequency (43), we calculated the normalized ratio of nonsynonymous to synonymous mutations (dN/dS). Although dN/dS ratios can approach 1.0 when selection is ineffective (complete relaxation of selection), values larger than 1.0 are only expected under adaptive evolution (text S2) (38, 44). We found that dN/dS ratios increased with inversion correlation, with highly positive ICS showing dN/dS ≥ 1 for all five chromosomes (Fig. 4B and table S15). We confirmed with evolutionary simulations that such a pattern is only

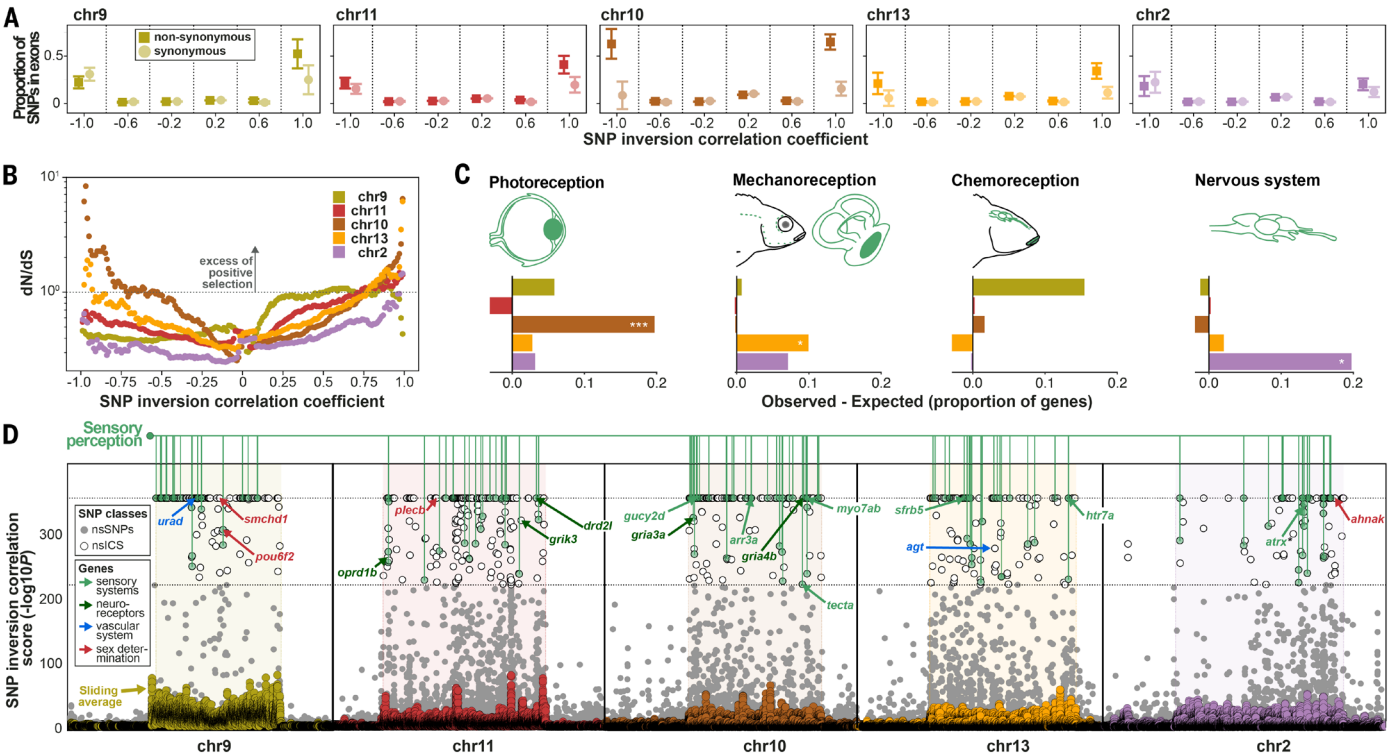


Fig. 4. Adaptive evolution of inversion haplotypes. (A) Proportion of exonic SNPs, grouped by inversion correlation coefficient intervals, relative to all SNPs within the same interval. A positive correlation coefficient corresponds to the derived SNP allele being more common on the inverted haplotype, whereas a negative coefficient corresponds to the derived SNP allele being more common on the noninverted haplotype (ancestral orientation). (B) dN/dS measured for SNPs as a function of inversion genotype correlation [see materials and methods (38)]. (C) Excess of genes containing nsICs among all genes highly expressed in the main sensory (green) and nervous system (blue). Expression data are based on the single-cell expression atlas of developing zebrafish *Danio*cell (45). The tissues were grouped into the functional categories: vision (eye), mechanoreception (lateral line, ear), chemoreception (taste, olfaction), and nervous system (neural). (D) Nonsynonymous SNPs (nsSNPs, gray dots; if ICS, empty dots) and averaged ICS scores in 100 SNP rolling windows (markers are color-coded according to inversion) on the five inversion chromosomes. We annotated nsICs located in genes with high expression in zebrafish tissue groups related to sensory perception [same as in (C)]. nsICs in candidate genes discussed in the main text are annotated with arrows (if several were located in the same gene, the highest nsIC is annotated) and color coded by functional category (table S24).

expected in the presence of substantial numbers of positively selected variants (text S2 and figs. S44 and S45) (38). Therefore, we conclude that widespread adaptive evolution contributed to diversification between ancestral and inverted haplotypes on all five chromosomes.

Despite their general high differentiation, for many ICS, both alleles were present in at least one copy on both inverted and noninverted haplotypes (37 to 72% of ICS; table S16). As expected, this pattern of shared polymorphism across inversion orientations is even more apparent for other (non-ICS) common variants (table S16) and suggests that, despite their excess divergence, recombination between inversion region haplotypes is not uncommon at evolutionary timescales, potentially providing a mechanism to concentrate adaptive alleles on such haplotypes.

Inversions contribute to sensory and physiological adaptation

To study functional roles of genes involved in inversion adaptations, we first analyzed expression of the 315 genes from inversion regions with nonsynonymous ICS (nsICs) in a multitissue single-cell gene expression atlas of the zebrafish model [*Danio*cell database (45) and text S3] (38). We found that individual inversions showed elevated expression in tissues related to vision, mechanoreception, and the nervous system [false discovery rate (FDR)-corrected $P = 2 \times 10^{-4}$, 0.02, and 0.04, respectively] (Fig. 4C, figs. S46 and S47, and tables S17 to S20). As most of the associations were related to neural and sensory tissues, we checked for overrepresentation of all neural and sensory tissues across all five inversions and found them to be significant (FDR-corrected $P = 6 \times 10^{-4}$; fig. S48 and tables S21 and S22). We additionally tested

for gene ontology enrichment of genes near ICS [see materials and methods; (38)] and found sensory system-related categories in all five inversions (table S23). Lastly, we found vascular system-related categories functionally linked to responses to hypoxia stress to be enriched in three inversions. All these findings are consistent with adaptations related to changes in light, oxygen, and hydrostatic pressure along a depth gradient, as observed in many aquatic organisms (46–48), including cichlids (31, 49, 50).

Among the 83 genes with two or more nsICs were strong candidate genes for depth adaptation (tables S24 and S25), including genes involved in signal transduction in photoreceptor cells (*arr3a*, *gucy2d*, and *pou6f2*), otolith tethering (*tecta*), sound perception (*myo7ab*), kidney function and blood pressure regulation (*ura*d), and a master regulator of vasoconstriction (*agt*) (Fig. 4D, table S24, and text S4) (38). Notably, some genes showed a close similarity between the amino acid sequence coded by the inverted haplotype and that of *Diplotaxodon*, even when the relevant inversion was not present in *Diplotaxodon* [e.g., *arr3a* on chromosome 10; see also Malinsky *et al.* (31)] (fig. S49), which is consistent with a hybrid ancestry of benthics and subsequent differential selection between recombination-suppressed inversion haplotypes. Several genes harbor both positive and negative ICS, as expected under diversifying selection.

Consistent with their enrichment among sensory and neural tissues, we also found nsICs to be significantly overrepresented among neuroreceptor genes that have been previously associated with social (glutamate) and affiliative (oxytocin and arginine vasopressin or vasotocin, opioid receptors, dopamine, serotonin) behavior (51) (6 of the 46

candidate genes, Fisher's exact test $P = 0.0011$) (table S26). These are three glutamate receptors (*gria3a* and *gria4b* on chromosome 10 and *grik3* on chromosome 11), one opioid receptor (*oprd1b* on chromosome 11), one dopamine receptor (*drd2l* on chromosome 11), and one serotonin receptor (*htr7a* on chromosome 13) (fig. S49).

It is notable that the identified neurotransmitters are not only associated with fish social behavior in general but have been specifically associated with bower building behavior in Malawi cichlids (52), a behavioral phenotype important for assortative mating (53), which has previously been linked to the existence of supergenes (51) and associated with genetic divergence peaks inside our chromosome 2 and 11 inversion regions (34). Following this up, we found no significant correlation between bower type and the presence of the five inversions when accounting for phylogeny (fig. S50 and table S27; see text S1) [see materials and methods; (38)], suggesting that previously detected associations might be due to phylogenetic confounding.

Our selection analyses suggest that widespread functional divergence in genes related to sensory, vascular, and nervous systems occurred during the early evolution of inversion haplotypes.

Inversions contribute to sex determination

Considering segregation patterns of inversion genotypes within species, we observed a notable excess of inversion heterozygotes for chromosomes 9, 10, and 11 (deviation from within-species Hardy-Weinberg equilibrium, $P < 10^{-4}$, 0.0048, and 0.0133, respectively). This pattern was most extreme for chromosome 9, for which, despite the presence of 77 heterozygous individuals across twelve species, not a

single homozygous ancestral (noninverted) state was present in any benthic.

Because inversions are a common feature in the evolution of suppressed recombination on sex chromosomes (54, 55), we hypothesized that the observed excess of heterozygotes could be due to sex-linked inheritance (fig. S51). In the two species for which we had gonad examination-based sex assignment, we found a perfect correlation of sex with chromosome 11 inversion state in *Copadichromis chrysonotus* (Fig. 5, A and B) ($n = 28$ individuals, Fisher's exact test $P = 4.7 \times 10^{-8}$), whereas the other species, *Copadichromis mloto*, was not variable for any inversion. We further confirmed a significant chromosome 11 inversion: sex association among 107 laboratory-bred individuals from 11 broods of three species (Fig. 5, C to E). However, in a second laboratory population of one of these species (*Otopharynx tetrastigma*) with different geographic origin, the chromosome 11 inversion was fixed for the inverted state, but there was a correlation of sex with the chromosome 9 inversion state (Fig. 5E). This is consistent with previous observations of multiple sex determination systems acting even within single Malawi cichlid species (56, 57). In each case where there was an association, males tended to be heterozygous and females, homozygous, for the respective inverted state, as expected for XY-like sex determination systems.

To further examine the extent of sex linkage of inversions, we pooled data for each inversion across species with at least one heterozygous sample (table S28). This revealed that, whereas females tended to be homozygous for the inverted state, there was a significant association of male sex with the heterozygous state for chromosomes 9, 10, and 11

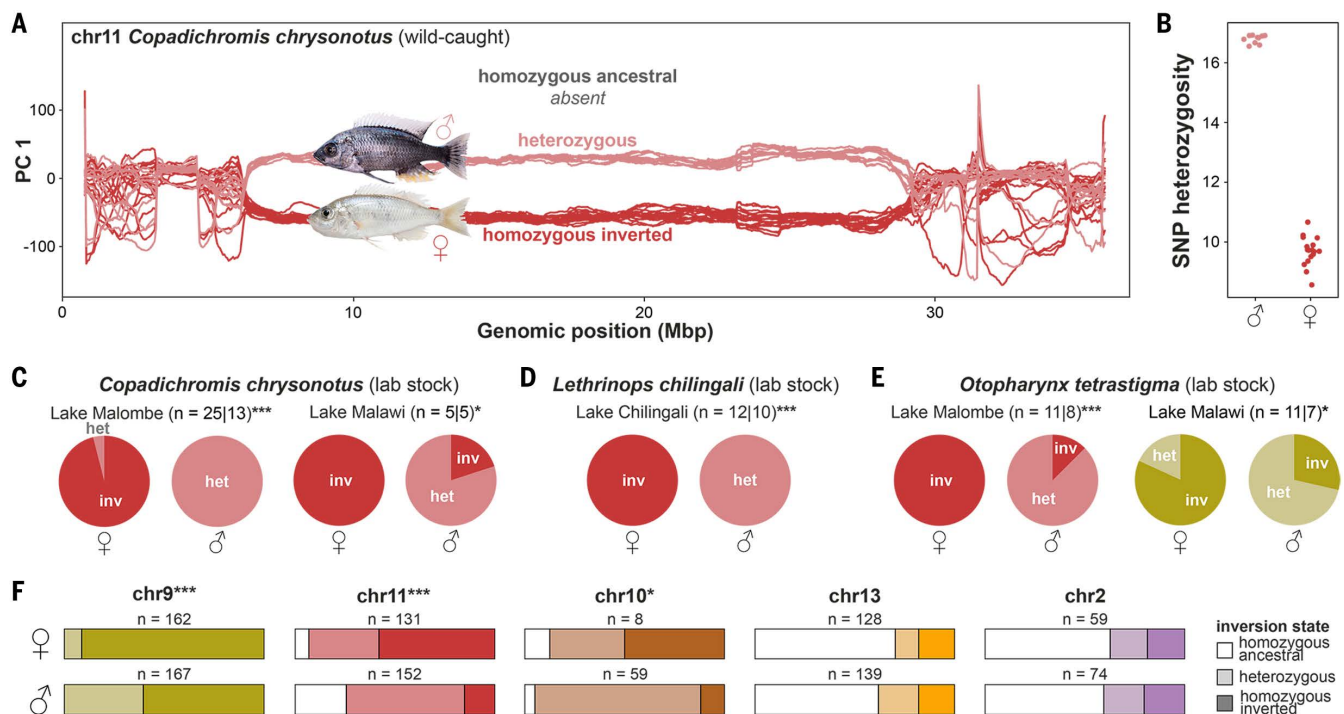


Fig. 5. Sex association of inversions. (A) Windowed PC analysis along chromosome 11 demonstrates perfect association of inversion genotype with sex in our sample of 28 wild-caught *C. chrysonotus*. (B) SNP heterozygosity among our sample of wild-caught male and female *C. chrysonotus*, measured as number of heterozygous SNPs per 10 kilo-base pairs. (C to E) Sex-inversion associations in lab-raised populations. Per population, the number of females and males is given (separated by a vertical line), and asterisks denote significance levels of Fisher's exact tests of inversion genotype–sex correlation (* $P < 0.05$; *** $P < 0.001$). Inversion genotype per sex (confirmed through gonad examination) in lab-raised broods of (C) *C. chrysonotus* from Lake Malombe ($P < 0.001$, left) and from Lake Malawi ($P = 0.048$, right), (D) *Lethrinops chilingali* from satellite lake Chilingali ($P < 0.001$), and (E) *O. tetrastigma* from Lake Malombe at the outflow of Lake Malawi ($P < 0.001$, left) and from the northern part of Lake Malawi ($P = 0.049$, right). het, heterozygous; inv, inverted. (F) Proportions of homozygous to heterozygous inversion genotypes in males and females of species with heterozygotes present, according to WGS and PCR typing of 809 samples (67 species). Asterisks denote significance levels of Fisher's exact tests of inversion genotype–sex correlation (* $P < 0.05$; *** $P < 0.001$).

(Fisher's exact test $P = 3.7 \times 10^{-11}$, 0.014, and 5.3×10^{-11} , respectively) (Fig. 5F and table S28), consistent with a widespread role of the inversions in sex determination. That said, many species were not polymorphic for inversions, and, even within polymorphic species, associations were usually not perfect (data S3), suggesting additional genetic or environmental effects contributing to sex determination and a rapid turnover of sex-linked function.

Given that the evolution of sex-determining regions often involves changes in gene expression between male and female haplotypes, we obtained transcriptomic data of five tissues (muscle, liver, brain, gills, and gonads) for 11 males of *C. chrysonotus*—the species in which males were heterozygous for the chromosome 11 inversion, whereas females were fixed for the inverted state—and investigated allele-specific expression (ASE). Among genes with significant ASE (fig. S52 and text S3) (38), there was a moderate bias toward lower expression of the Y-like noninverted haplotype, a pattern seen in many organisms (58). Further, lacking access to appropriate female samples, we obtained equivalent data for 11 male *C. mloto*, the congeneric species fixed for the derived chromosome 11 inversion state, to perform differential gene expression (DE) analysis between the two inversion states (fig. S53). Several of the significant ASE and DE genes ($FDR < 0.05$) were implicated in sex determination, sex specific expression, or gonad function in other (fish) species (table S24) and ICS were significantly overrepresented among genes with significant allele specific expression (Fisher's exact test $P = 1.6 \times 10^{-7}$). Furthermore, we found candidate genes related to sex and reproduction among the strongest candidate genes for adaptive evolution (i.e., those with the largest number of nsICs) (Fig. 4D and text S3) (38).

It is notable that, for each of the three inversions with evidence for sex-linkage, the Y-like, noninverted haplotype arrived in the affected benthics through introgression events, affecting mainly eukambuzi, other shallow benthics and utaka, and deep benthics for chromosomes 9, 11, and 10, respectively (events @, ©, and ©, Fig. 3B). For chromosome 9, this is further supported by results from a lab based hybrid cross between females of *A. calliptera* and males of the eukambuzi *Protomelas taeniolatus*, which showed a quantitative trait locus (QTL) peak for sex in the chromosome 9 inversion region (59). This is consistent with a dominant male-determining function of the noninverted benthic haplotype (with origin external to the Malawi radiation) even when paired with an *A. calliptera* haplotype of the same orientation.

To further investigate the generality of the role of inversions in sex determination of haplochromine cichlids, we applied our SNP-based inversion detection approach to publicly available sequencing data for the Lake Victoria adaptive radiation (60). The results suggest that the sex-linked regions identified by Feller *et al.* (59) on chromosomes 9 and 23 are in fact chromosomal inversions (the one on chromosome 9 being distinct from the one present in Malawi) (figs. S22 and S54), pointing to a wider relevance of chromosomal inversions in cichlid sex determination.

Discussion

In this study, we identified large chromosomal inversions present in the Lake Malawi cichlid radiation and present evidence that their evolutionary history was shaped by introgression, ecological adaptation, and the turnover of sex determination systems. Our results are consistent with a recent preprint that independently identified the inversions described here and their sex linkage based on optical mapping and chromosome-level de novo assemblies (61). Given the evolutionarily independent presence of sex-linked inversions in Lake Victoria cichlids (fig. S54), which are potentially also involved in adaptive introgression (60), and large-scale differences between the genomes of male and female Lake Tanganyika cichlids (62), we suggest that such rearrangements may be a common feature of adaptive radiation in cichlids.

Chromosomal inversions have been implicated in adaptation, sex determination, and speciation in many systems, especially in the context

of adaptive divergence with gene flow (7, 11, 15–22, 28) likely because of their ability to lock together adaptive alleles (7). The chromosomal inversions that we identified in Malawi cichlids were involved in gene flow events at different stages of the radiation, most prominently a founding admixture event of the species-rich benthic clade and introgression from a distantly related lineage outside the Malawi radiation (chromosome 9 inversion). These events coincide with bursts of ecomorphological diversification of the resulting lineages. In the latter case, this concerns the eukambuzi, which show exceptional diversity in ecomorphology, body patterning, and coloration (30).

We found evidence for inversion transmission between deep and shallow benthic species caught at similar depths (fig. S35). At the same time, when not introgressed, inversions seemingly helped to suppress gene flow and thereby contributed to adaptive divergence. However, despite their excess divergence compared with the rest of the genome and the complete recombination suppression that we observed in a cross (Fig. 2E), most common genetic polymorphism is shared across orientations, suggesting that inversions are a barrier to genetic exchange rather than completely suppressing it. On one hand, this facilitates the purging of genetic load, which often hinders the spread of inversions (63); on the other hand, it provides an additional mechanism for the creation of combinatorial diversity (5).

The genetic variants most differentiated between inverted and non-inverted haplotypes (ICS) show a strong relative excess of amino acid changing mutations, as expected only under adaptive evolution at many loci (text S3) (38). These mutations showed enrichment in genes related to and expressed in tissues involved in sensory and behavioral functions. This makes sense because sensory systems mediate sound perception, mechanoreception, and vision, essential for navigation and feeding in fishes (64), making them important targets of ecological adaptation to differing underwater environments (65). Although further experiments—most promisingly, within species polymorphic for inversions—will be necessary to dissect the precise phenotypes of the adaptive alleles within inversion regions, our results point toward widespread, multigenic adaptation along a depth gradient, which is a frequent axis of differentiation in fishes (49, 66).

We found evidence for XY-like sex linkage of the inversions on chromosomes 9, 10, and 11 in which introgressed haplotypes of ancestral orientation act as Y chromosomes in some extant species, with inversion-region genes related to sex and reproduction being under allele specific expression in XY males and showing signatures of selection. Consistent with the highly dynamic nature of sex determination in many fishes (67) and, specifically, cichlids (59, 62, 68), our results point to a relatively easy recruitment of sex determination loci (SDLs), possibly as a direct consequence of introgression of relatively divergent haplotypes affecting a sex determination threshold, or owing to heterozygote advantage of introgressed inversions selecting for the recruitment of SDLs (69).

Sexual selection has been identified as a major predictor of successful radiation in cichlids (70), and assortative mating is a main driver of cichlid reproductive isolation (71). Both of these processes rely heavily on the same sensory systems [e.g., vision (71), olfaction (72), and hearing (73)] that are also relevant for adaptation to depth and feeding niches and that we identified as candidates for adaptive evolution. Assortative mating and the evolution of sex-linked regions are both forms of sex-specific selection (74). Although the interplay between these forms of selection is not well understood, it can give rise to synergistic evolutionary dynamics, potentially mediated by sexually antagonistic selection (75, 76).

Although our analysis focused on genetic variants nearly fixed between inversion haplotypes, we expect that additional variants specific to particular species groups will prove important for further diversification. Furthermore, alongside the inversions that identify admixture events, we also see a signal of introgressed material in the rest of the genome, providing a potential substrate for further selection and

adaptation. Indeed, although we focused on large inversions segregating across many species, there are expected to be many more inversions and other structural genetic variants that are smaller or have a more limited taxonomic distribution, as suggested by our whole genome alignments and in Talbi *et al.* (77). Surely, more structural variants with relevance in adaptive diversification are to be found in future studies.

In conclusion, the haplotypes of five chromosomal-scale inversions in the Malawi cichlid adaptive radiation show supergene-like signs of adaptive evolution and repeated introgression associated with speciation. Together with the repeated transient sex-linked nature of introgressed haplotypes, this provides a substrate for rich evolutionary dynamics around the interactions between natural, sexual, and sexually antagonistic selection.

Materials and methods are available in the supplementary materials.

REFERENCES AND NOTES

- N. Eldredge *et al.*, The dynamics of evolutionary stasis. *Paleobiology* **31** (sp5), 133–145 (2005). doi: [10.1666/0094-8373\(2005\)031\[0133:TDOES\]2.0.CO;2](https://doi.org/10.1666/0094-8373(2005)031[0133:TDOES]2.0.CO;2)
- D. Berner, W. Salzburger, The genomics of organismal diversification illuminated by adaptive radiations. *Trends Genet.* **31**, 491–499 (2015). doi: [10.1016/j.tig.2015.07.002](https://doi.org/10.1016/j.tig.2015.07.002); pmid: [26259669](https://pubmed.ncbi.nlm.nih.gov/26259669/)
- T. C. Nelson, W. A. Cresko, Ancient genomic variation underlies repeated ecological adaptation in young stickleback populations. *Evol. Lett.* **2**, 9–21 (2018). doi: [10.1002/evl3.37](https://doi.org/10.1002/evl3.37); pmid: [30283661](https://pubmed.ncbi.nlm.nih.gov/30283661/)
- J. I. Meier *et al.*, Ancient hybridization fuels rapid cichlid fish adaptive radiations. *Nat. Commun.* **8**, 14363 (2017). doi: [10.1038/ncomms14363](https://doi.org/10.1038/ncomms14363); pmid: [28186104](https://pubmed.ncbi.nlm.nih.gov/28186104/)
- D. A. Marques, J. I. Meier, O. Seehausen, A Combinatorial View on Speciation and Adaptive Radiation. *Trends Ecol. Evol.* **34**, 531–544 (2019). doi: [10.1016/j.tree.2019.02.008](https://doi.org/10.1016/j.tree.2019.02.008); pmid: [30885412](https://pubmed.ncbi.nlm.nih.gov/30885412/)
- D. Roze, N. H. Barton, The Hill-Robertson effect and the evolution of recombination. *Genetics* **173**, 1793–1811 (2006). doi: [10.1534/genetics.106.058586](https://doi.org/10.1534/genetics.106.058586); pmid: [16702422](https://pubmed.ncbi.nlm.nih.gov/16702422/)
- M. Kirkpatrick, N. Barton, Chromosome inversions, local adaptation and speciation. *Genetics* **173**, 419–434 (2006). doi: [10.1534/genetics.105.047985](https://doi.org/10.1534/genetics.105.047985); pmid: [16204214](https://pubmed.ncbi.nlm.nih.gov/16204214/)
- A. Akerman, R. Bürger, The consequences of gene flow for local adaptation and differentiation: A two-locus two-deme model. *J. Math. Biol.* **68**, 1135–1198 (2014). doi: [10.1007/s00285-013-0660-z](https://doi.org/10.1007/s00285-013-0660-z); pmid: [23532261](https://pubmed.ncbi.nlm.nih.gov/23532261/)
- R. K. Butlin, Recombination and speciation. *Mol. Ecol.* **14**, 2621–2635 (2005). doi: [10.1111/j.1365-294X.2005.02617.x](https://doi.org/10.1111/j.1365-294X.2005.02617.x); pmid: [16029465](https://pubmed.ncbi.nlm.nih.gov/16029465/)
- M. Kirkpatrick, How and why chromosome inversions evolve. *PLOS Biol.* **8**, e1000501 (2010). doi: [10.1371/journal.pbio.1000501](https://doi.org/10.1371/journal.pbio.1000501); pmid: [20927412](https://pubmed.ncbi.nlm.nih.gov/20927412/)
- M. Wellenreuther, L. Bernatchez, Eco-Evolutionary Genomics of Chromosomal Inversions. *Trends Ecol. Evol.* **33**, 427–440 (2018). doi: [10.1016/j.tree.2018.04.002](https://doi.org/10.1016/j.tree.2018.04.002); pmid: [29731154](https://pubmed.ncbi.nlm.nih.gov/29731154/)
- M. Kirkpatrick, B. Barrett, Chromosome inversions, adaptive cassettes and the evolution of species' ranges. *Mol. Ecol.* **24**, 2046–2055 (2015). doi: [10.1111/mec.13074](https://doi.org/10.1111/mec.13074); pmid: [25583098](https://pubmed.ncbi.nlm.nih.gov/25583098/)
- E. R. Hager *et al.*, A chromosomal inversion contributes to divergence in multiple traits between deer mouse ecotypes. *Science* **377**, 399–405 (2022). doi: [10.1126/science.abg0718](https://doi.org/10.1126/science.abg0718); pmid: [35862520](https://pubmed.ncbi.nlm.nih.gov/35862520/)
- F. C. Jones *et al.*, The genomic basis of adaptive evolution in threespine sticklebacks. *Nature* **484**, 55–61 (2012). doi: [10.1038/nature10944](https://doi.org/10.1038/nature10944); pmid: [22481358](https://pubmed.ncbi.nlm.nih.gov/22481358/)
- R. Faria, A. Navarro, Chromosomal speciation revisited: Rearranging theory with pieces of evidence. *Trends Ecol. Evol.* **25**, 660–669 (2010). doi: [10.1016/j.tree.2010.07.008](https://doi.org/10.1016/j.tree.2010.07.008); pmid: [20817305](https://pubmed.ncbi.nlm.nih.gov/20817305/)
- D. Ayala, R. F. Guerrero, M. Kirkpatrick, Reproductive isolation and local adaptation quantified for a chromosome inversion in a malaria mosquito. *Evolution* **67**, 946–958 (2013). doi: [10.1111/j.1558-5646.2012.01836.x](https://doi.org/10.1111/j.1558-5646.2012.01836.x); pmid: [23550747](https://pubmed.ncbi.nlm.nih.gov/23550747/)
- M. Joron *et al.*, A conserved supergene locus controls colour pattern diversity in *Heliconius* butterflies. *PLOS Biol.* **4**, e303 (2006). doi: [10.1371/journal.pbio.0040303](https://doi.org/10.1371/journal.pbio.0040303); pmid: [17002517](https://pubmed.ncbi.nlm.nih.gov/17002517/)
- K. Kunte *et al.*, doublesex is a mimicry supergene. *Nature* **507**, 229–232 (2014). doi: [10.1038/nature13112](https://doi.org/10.1038/nature13112); pmid: [24598547](https://pubmed.ncbi.nlm.nih.gov/24598547/)
- C. Küpper *et al.*, A supergene determines highly divergent male reproductive morphs in the ruff. *Nat. Genet.* **48**, 79–83 (2016). doi: [10.1038/ng.3443](https://doi.org/10.1038/ng.3443); pmid: [26569125](https://pubmed.ncbi.nlm.nih.gov/26569125/)
- J. Wang *et al.*, A Y-like social chromosome causes alternative colony organization in fire ants. *Nature* **493**, 664–668 (2013). doi: [10.1038/nature11832](https://doi.org/10.1038/nature11832); pmid: [23334415](https://pubmed.ncbi.nlm.nih.gov/23334415/)
- P. R. Berg *et al.*, Three chromosomal rearrangements promote genomic divergence between migratory and stationary ecotypes of Atlantic cod. *Sci. Rep.* **6**, 23246 (2016). doi: [10.1038/srep23246](https://doi.org/10.1038/srep23246); pmid: [26983361](https://pubmed.ncbi.nlm.nih.gov/26983361/)
- M. A. F. Noor, K. L. Grams, L. A. Bertucci, J. Reiland, Chromosomal inversions and the reproductive isolation of species. *Proc. Natl. Acad. Sci. U.S.A.* **98**, 12084–12088 (2001). doi: [10.1073/pnas.221274498](https://doi.org/10.1073/pnas.221274498); pmid: [11593019](https://pubmed.ncbi.nlm.nih.gov/11593019/)
- R. Castiglia, Sympatric sister species in rodents are more chromosomally differentiated than allopatric ones: Implications for the role of chromosomal rearrangements in speciation. *Mammal Rev.* **44**, 1–4 (2014). doi: [10.1111/mam.12009](https://doi.org/10.1111/mam.12009)
- D. M. Hooper, T. D. Price, Chromosomal inversion differences correlate with range overlap in passerine birds. *Nat. Ecol. Evol.* **1**, 1526–1534 (2017). doi: [10.1038/s41559-017-0284-6](https://doi.org/10.1038/s41559-017-0284-6); pmid: [29185507](https://pubmed.ncbi.nlm.nih.gov/29185507/)
- C.-J. Rubin *et al.*, Rapid adaptive radiation of Darwin's finches depends on ancestral genetic modules. *Sci. Adv.* **8**, eabm5982 (2022). doi: [10.1126/sciadv.abm5982](https://doi.org/10.1126/sciadv.abm5982); pmid: [35857449](https://pubmed.ncbi.nlm.nih.gov/35857449/)
- D. Brawand *et al.*, The genomic substrate for adaptive radiation in African cichlid fish. *Nature* **513**, 375–381 (2014). doi: [10.1038/nature13726](https://doi.org/10.1038/nature13726); pmid: [25186727](https://pubmed.ncbi.nlm.nih.gov/25186727/)
- E. D. Enbody *et al.*, Community-wide genome sequencing reveals 30 years of Darwin's finch evolution. *Science* **381**, eadf6218 (2023). doi: [10.1126/science.adf6218](https://doi.org/10.1126/science.adf6218); pmid: [37769091](https://pubmed.ncbi.nlm.nih.gov/37769091/)
- U. Knief *et al.*, Evolution of Chromosomal Inversions across an Avian Radiation. *Mol. Biol. Evol.* **41**, msae092 (2024). doi: [10.1093/molbev/msae092](https://doi.org/10.1093/molbev/msae092); pmid: [38743589](https://pubmed.ncbi.nlm.nih.gov/38743589/)
- G. Barlow, "The Cichlid Fishes: Nature's Grand Experiment" in *Evolution* (Perseus Books Group, 2000).
- A. Konings, *Malawi Cichlids in Their Natural Habitat* (Cichlid Press, 2016).
- M. Malinsky *et al.*, Whole-genome sequences of Malawi cichlids reveal multiple radiations interconnected by gene flow. *Nat. Ecol. Evol.* **2**, 1940–1955 (2018). doi: [10.1038/s41559-018-0717-x](https://doi.org/10.1038/s41559-018-0717-x); pmid: [30455444](https://pubmed.ncbi.nlm.nih.gov/30455444/)
- H. Svardal *et al.*, Ancestral Hybridization Facilitated Species Diversification in the Lake Malawi Cichlid Fish Adaptive Radiation. *Mol. Biol. Evol.* **37**, 1100–1113 (2020). doi: [10.1093/molbev/msz294](https://doi.org/10.1093/molbev/msz294); pmid: [31821500](https://pubmed.ncbi.nlm.nih.gov/31821500/)
- R. B. Stelkens, C. Schmid, O. Selz, O. Seehausen, Phenotypic novelty in experimental hybrids is predicted by the genetic distance between species of cichlid fish. *BMC Evol. Biol.* **9**, 283 (2009). doi: [10.1186/1471-2148-9-283](https://doi.org/10.1186/1471-2148-9-283); pmid: [19961584](https://pubmed.ncbi.nlm.nih.gov/19961584/)
- R. A. York *et al.*, Behavior-dependent cis regulation reveals genes and pathways associated with bower building in cichlid fishes. *Proc. Natl. Acad. Sci. U.S.A.* **115**, E11081–E11090 (2018). doi: [10.1073/pnas.1810140115](https://doi.org/10.1073/pnas.1810140115); pmid: [30397142](https://pubmed.ncbi.nlm.nih.gov/30397142/)
- M. A. Conte *et al.*, Chromosome-scale assemblies reveal the structural evolution of African cichlid genomes. *Gigascience* **8**, giz030 (2019). doi: [10.1093/gigascience/giz030](https://doi.org/10.1093/gigascience/giz030); pmid: [30942871](https://pubmed.ncbi.nlm.nih.gov/30942871/)
- O. S. Harringmeyer, H. E. Hoekstra, Chromosomal inversion polymorphisms shape the genomic landscape of deer mice. *Nat. Ecol. Evol.* **6**, 1965–1979 (2022). doi: [10.1038/s41559-022-01890-0](https://doi.org/10.1038/s41559-022-01890-0); pmid: [36253543](https://pubmed.ncbi.nlm.nih.gov/36253543/)
- P. Jay *et al.*, Mutation load at a mimicry supergene sheds new light on the evolution of inversion polymorphisms. *Nat. Genet.* **53**, 288–293 (2021). doi: [10.1038/s41588-020-00771-1](https://doi.org/10.1038/s41588-020-00771-1); pmid: [33495598](https://pubmed.ncbi.nlm.nih.gov/33495598/)
- Materials and methods are available as supplementary materials.
- A. Rhie *et al.*, Towards complete and error-free genome assemblies of all vertebrate species (Cold Spring Harbor Laboratory, 2020), p. 2020.05.22.110833.
- H. Li, P. Ralph, Local PCA Shows How the Effect of Population Structure Differs Along the Genome. *Genetics* **211**, 289–304 (2019). doi: [10.1534/genetics.118.301747](https://doi.org/10.1534/genetics.118.301747); pmid: [30459280](https://pubmed.ncbi.nlm.nih.gov/30459280/)
- L. S. Stevison, K. B. Hoehn, M. A. F. Noor, Effects of inversions on within- and between-species recombination and divergence. *Genome Biol. Evol.* **3**, 830–841 (2011). doi: [10.1093/gbe/evr081](https://doi.org/10.1093/gbe/evr081); pmid: [21828374](https://pubmed.ncbi.nlm.nih.gov/21828374/)
- N. Patterson *et al.*, Ancient admixture in human history. *Genetics* **192**, 1065–1093 (2012). doi: [10.1534/genetics.112.145037](https://doi.org/10.1534/genetics.112.145037); pmid: [22960212](https://pubmed.ncbi.nlm.nih.gov/22960212/)
- N. Galtier, Half a Century of Controversy: The Neutralist/Selectionist Debate in Molecular Evolution. *Genome Biol. Evol.* **16**, evae003 (2024). doi: [10.1093/gbe/evae003](https://doi.org/10.1093/gbe/evae003); pmid: [38311843](https://pubmed.ncbi.nlm.nih.gov/38311843/)
- M. W. Hahn, *Molecular Population Genetics* (Sinauer Associates, Incorporated, 2018).
- A. Sur, Y. Wang, P. Capar, G. Margolin, J. A. Farrell, Single-cell analysis of shared signatures and transcriptional diversity during zebrafish development. *bioRxiv* 2023.03.20.533545 [Preprint] (2023); <https://doi.org/10.1101/2023.03.20.533545>
- Z. Musilova *et al.*, Vision using multiple distinct rod opsins in deep-sea fishes. *Science* **364**, 588–592 (2019). doi: [10.1126/science.aav4632](https://doi.org/10.1126/science.aav4632); pmid: [31073066](https://pubmed.ncbi.nlm.nih.gov/31073066/)
- A. Brown, S. Thatje, Explaining bathymetric diversity patterns in marine benthic invertebrates and demersal fishes: Physiological contributions to adaptation of life at depth. *Biol. Rev. Camb. Philos. Soc.* **89**, 406–426 (2014). doi: [10.1111/brv.12061](https://doi.org/10.1111/brv.12061); pmid: [24118851](https://pubmed.ncbi.nlm.nih.gov/24118851/)
- H.-S. Yim *et al.*, Minke whale genome and aquatic adaptation in cetaceans. *Nat. Genet.* **46**, 88–92 (2014). doi: [10.1038/ng.2835](https://doi.org/10.1038/ng.2835); pmid: [24270359](https://pubmed.ncbi.nlm.nih.gov/24270359/)
- M. Malinsky *et al.*, Genomic islands of speciation separate cichlid ecomorphs in an East African crater lake. *Science* **350**, 1493–1498 (2015). doi: [10.1126/science.aac9927](https://doi.org/10.1126/science.aac9927); pmid: [26680190](https://pubmed.ncbi.nlm.nih.gov/26680190/)
- C. Hahn, M. J. Genner, G. F. Turner, D. A. Joyce, The genomic basis of cichlid fish adaptation within the deepwater "twilight zone" of Lake Malawi. *Evol. Lett.* **1**, 184–198 (2017). doi: [10.1002/evl3.20](https://doi.org/10.1002/evl3.20); pmid: [30283648](https://pubmed.ncbi.nlm.nih.gov/30283648/)

51. S. L. Mederos *et al.*, Effects of pairing on color change and central gene expression in lined seahorses. *Genes Brain Behav.* **21**, e12812 (2022). doi: [10.1111/gbb.12812](https://doi.org/10.1111/gbb.12812); pmid: [35652318](https://pubmed.ncbi.nlm.nih.gov/35652318/)
52. Z. V. Johnson *et al.*, Cellular profiling of a recently-evolved social behavior in cichlid fishes. *Nat. Commun.* **14**, 4891 (2023). doi: [10.1038/s41467-023-40331-9](https://doi.org/10.1038/s41467-023-40331-9); pmid: [37580322](https://pubmed.ncbi.nlm.nih.gov/37580322/)
53. I. S. Magalhaes, A. M. Smith, D. A. Joyce, Quantifying mating success of territorial males and sneakers in a bower-building cichlid fish. *Sci. Rep.* **7**, 41128 (2017). doi: [10.1038/srep41128](https://doi.org/10.1038/srep41128); pmid: [28128313](https://pubmed.ncbi.nlm.nih.gov/28128313/)
54. D. Bachtrog, Y-chromosome evolution: Emerging insights into processes of Y-chromosome degeneration. *Nat. Rev. Genet.* **14**, 113–124 (2013). doi: [10.1038/nrg3366](https://doi.org/10.1038/nrg3366); pmid: [23329112](https://pubmed.ncbi.nlm.nih.gov/23329112/)
55. C. L. Peichel *et al.*, Assembly of the threespine stickleback Y chromosome reveals convergent signatures of sex chromosome evolution. *Genome Biol.* **21**, 177 (2020). doi: [10.1186/s13059-020-02097-x](https://doi.org/10.1186/s13059-020-02097-x); pmid: [32684159](https://pubmed.ncbi.nlm.nih.gov/32684159/)
56. J. R. Ser, R. B. Roberts, T. D. Kocher, Multiple interacting loci control sex determination in lake Malawi cichlid fish. *Evolution* **64**, 486–501 (2010). doi: [10.1111/j.1558-5646.2009.00871.x](https://doi.org/10.1111/j.1558-5646.2009.00871.x); pmid: [19863587](https://pubmed.ncbi.nlm.nih.gov/19863587/)
57. H. Munby *et al.*, Differential use of multiple genetic sex determination systems in divergent ecomorphs of an African crater lake cichlid, bioRxiv 2021.08.05.455235 [Preprint] (2021); <https://doi.org/10.1101/2021.08.05.455235>.
58. Q. Zhou, D. Bachtrog, Chromosome-wide gene silencing initiates Y degeneration in *Drosophila*. *Curr. Biol.* **22**, 522–525 (2012). doi: [10.1016/j.cub.2012.01.057](https://doi.org/10.1016/j.cub.2012.01.057); pmid: [22365853](https://pubmed.ncbi.nlm.nih.gov/22365853/)
59. A. F. Feller, V. Ogi, O. Seehausen, J. I. Meier, Identification of a novel sex determining chromosome in cichlid fishes that acts as XY or ZW in different lineages. *Hydrobiologia* **848**, 3727–3745 (2021). doi: [10.1007/s10750-021-04560-7](https://doi.org/10.1007/s10750-021-04560-7); pmid: [34720170](https://pubmed.ncbi.nlm.nih.gov/34720170/)
60. M. D. McGee *et al.*, The ecological and genomic basis of explosive adaptive radiation. *Nature* **586**, 75–79 (2020). doi: [10.1038/s41586-020-2652-7](https://doi.org/10.1038/s41586-020-2652-7); pmid: [32848251](https://pubmed.ncbi.nlm.nih.gov/32848251/)
61. N. M. Kumar, T. L. Cooper, T. D. Kocher, J. T. Streelman, P. T. McGrath, Large inversions in Lake Malawi cichlids are associated with habitat preference, lineage, and sex determination. *eLife* **14**, RP104923 (2025). pmid: [39554119](https://pubmed.ncbi.nlm.nih.gov/39554119/)
62. A. El Taher, F. Ronco, M. Matschiner, W. Salzburger, A. Böhne, Dynamics of sex chromosome evolution in a rapid radiation of cichlid fishes. *Sci. Adv.* **7**, eabe8215 (2021). doi: [10.1126/sciadv.abe8215](https://doi.org/10.1126/sciadv.abe8215); pmid: [34516923](https://pubmed.ncbi.nlm.nih.gov/34516923/)
63. E. L. Berdan, A. Blanckaert, R. K. Butlin, C. Bank, Deleterious mutation accumulation and the long-term fate of chromosomal inversions. *PLOS Genet.* **17**, e1009411 (2021). doi: [10.1371/journal.pgen.1009411](https://doi.org/10.1371/journal.pgen.1009411); pmid: [33661924](https://pubmed.ncbi.nlm.nih.gov/33661924/)
64. D. Escobar-Camacho, K. L. Carleton, Sensory modalities in cichlid fish behavior. *Curr. Opin. Behav. Sci.* **6**, 115–124 (2015). doi: [10.1016/j.cobeha.2015.11.002](https://doi.org/10.1016/j.cobeha.2015.11.002); pmid: [26693169](https://pubmed.ncbi.nlm.nih.gov/26693169/)
65. Z. Musilova, W. Salzburger, F. Cortesi, The Visual Opsin Gene Repertoires of Teleost Fishes: Evolution, Ecology, and Function. *Annu. Rev. Cell Dev. Biol.* **37**, 441–468 (2021). doi: [10.1146/annurev-cellbio-120219-024915](https://doi.org/10.1146/annurev-cellbio-120219-024915); pmid: [34351785](https://pubmed.ncbi.nlm.nih.gov/34351785/)
66. M. Barluenga, K. N. Stölting, W. Salzburger, M. Muschick, A. Meyer, Sympatric speciation in Nicaraguan crater lake cichlid fish. *Nature* **439**, 719–723 (2006). doi: [10.1038/nature04325](https://doi.org/10.1038/nature04325); pmid: [16467837](https://pubmed.ncbi.nlm.nih.gov/16467837/)
67. J. Kitano *et al.*, A Cryptic Sex-Linked Locus Revealed by the Elimination of a Master Sex-Determining Locus in Medaka Fish. *Am. Nat.* **202**, 231–240 (2023). doi: [10.1086/724840](https://doi.org/10.1086/724840); pmid: [37531272](https://pubmed.ncbi.nlm.nih.gov/37531272/)
68. W. J. Gammerding, T. D. Kocher, Unusual Diversity of Sex Chromosomes in African Cichlid Fishes. *Genes* **9**, 480 (2018). doi: [10.3390/genes9100480](https://doi.org/10.3390/genes9100480); pmid: [30287777](https://pubmed.ncbi.nlm.nih.gov/30287777/)
69. P. Jay, E. Tezenas, A. Véber, T. Giraud, Sheltering of deleterious mutations explains the stepwise extension of recombination suppression on sex chromosomes and other supergenes. *PLOS Biol.* **20**, e3001698 (2022). doi: [10.1371/journal.pbio.3001698](https://doi.org/10.1371/journal.pbio.3001698); pmid: [35853091](https://pubmed.ncbi.nlm.nih.gov/35853091/)
70. C. E. Wagner, L. J. Harmon, O. Seehausen, Ecological opportunity and sexual selection together predict adaptive radiation. *Nature* **487**, 366–369 (2012). doi: [10.1038/nature11144](https://doi.org/10.1038/nature11144); pmid: [22722840](https://pubmed.ncbi.nlm.nih.gov/22722840/)
71. O. M. Selz, M. E. R. Pierotti, M. E. Maan, C. Schmid, O. Seehausen, Female preference for male color is necessary and sufficient for assortative mating in 2 cichlid sister species. *Behav. Ecol.* **25**, 612–626 (2014). doi: [10.1093/beheco/aru024](https://doi.org/10.1093/beheco/aru024)
72. M. Plenderleith, C. van Oosterhout, R. L. Robinson, G. F. Turner, Female preference for conspecific males based on olfactory cues in a Lake Malawi cichlid fish. *Biol. Lett.* **1**, 411–414 (2005). doi: [10.1098/rsbl.2005.0355](https://doi.org/10.1098/rsbl.2005.0355); pmid: [17148220](https://pubmed.ncbi.nlm.nih.gov/17148220/)
73. K. P. Maruska, U. S. Ung, R. D. Fernald, The African cichlid fish *Astatotilapia burtoni* uses acoustic communication for reproduction: Sound production, hearing, and behavioral significance. *PLOS ONE* **7**, e37612 (2012). doi: [10.1371/journal.pone.0037612](https://doi.org/10.1371/journal.pone.0037612); pmid: [22624055](https://pubmed.ncbi.nlm.nih.gov/22624055/)
74. A. E. Wright, J. E. Mank, The scope and strength of sex-specific selection in genome evolution. *J. Evol. Biol.* **26**, 1841–1853 (2013). doi: [10.1111/jeb.12201](https://doi.org/10.1111/jeb.12201); pmid: [23848139](https://pubmed.ncbi.nlm.nih.gov/23848139/)
75. P. Muralidhar, Mating preferences of selfish sex chromosomes. *Nature* **570**, 376–379 (2019). doi: [10.1038/s41586-019-1271-7](https://doi.org/10.1038/s41586-019-1271-7); pmid: [31168095](https://pubmed.ncbi.nlm.nih.gov/31168095/)
76. S. H. Smith, K. Hsiung, A. Böhne, Evaluating the role of sexual antagonism in the evolution of sex chromosomes: New data from fish. *Curr. Opin. Genet. Dev.* **81**, 102078 (2023). doi: [10.1016/j.gde.2023.102078](https://doi.org/10.1016/j.gde.2023.102078); pmid: [37379742](https://pubmed.ncbi.nlm.nih.gov/37379742/)
77. M. Talbi, G. F. Turner, M. Malinsky, Rapid evolution of recombination landscapes during the divergence of cichlid ecotypes in Lake Masoko, bioRxiv 2024.03.20.585960 [Preprint] (2024); <https://doi.org/10.1101/2024.03.20.585960>.
78. R. Durbin *et al.*, Research data supporting “Introgression dynamics of sex-linked chromosomal inversions shape the Malawi cichlid radiation”, Apollo – University of Cambridge Repository (2025); <https://doi.org/10.17863/CAM.117242>.

ACKNOWLEDGMENTS

We thank the Department of Fisheries of the Government of Malawi for facilitating Malawi cichlid specimen collection; M. Genner, A. Tyers, M. Du, M. Mulumpwa, M. Nordborg, K. Svardal, and the staff of the Monkey Bay Fisheries Research Unit for support with sampling; S. McCarthy for bioinformatics support; W. Salzburger for access to facilities and data; and P. Gemmell for input on the project. We are grateful to D. Shaw, R. Schweiger, V. Caudill, P. Ralph, J. Lescroart, and E. De Keyser for useful comments on the manuscript. **Funding:** The authors gratefully acknowledge support through the Research Foundation – Flanders (FWO) (G047521N to H.S.), the Wellcome Trust (Wellcome grant 207492 to R.D., Wellcome Senior Investigator Award 219475/Z/19/Z to E.A.M.), the Research Fund of the University of Antwerp (BOF) (H.S.), the Cambridge-Africa ALBORADA Research Fund (H.S. and B.R.), the German Research Foundation (DFG) (492407022 and 497674620 to A.B.), the European Research Council (Proof-of-Concept grant 101069219 to M.K. and Y.F.C.), the Max Planck Society (Y.F.C.), and the Natural Environment Research Council (NERC) (IRF NE/R01504X/1 to M.E.S.). L.M.B. was supported through a Harding Distinguished Postgraduate Scholarship, and S.G. was supported through an FWO PhD Fellowship Fundamental Research. G.V. acknowledges Wolfson College University of Cambridge and the Genetics Society London for financial support. **Author contributions:** H.S. and R.D. conceived the study, with support from L.M.B. H.S. with R.D. organized cichlid collections in Malawi with support from B.R., R.Z., W.S., J.C.G., M.N., M.M., R.D., G.V., E.A.M., and G.F.T. G.F.T. undertook final taxonomic assignment. I.B. and V.B. performed DNA extractions. T.L. produced the original variant callset. H.S., L.M.B., V.B., I.A., J.S., and J.C.G. analyzed the SNP data. Inversion detection was accomplished by L.M.B. (PCA based) and I.A. (clusterization, phylogenetic reconstructions). H.S. performed hybridization analysis. V.B. made selection tests (together with H.S.), zebrafish-based functional analysis, and candidate genes investigation. J.C.G. performed enrichment analysis and candidate gene investigation. J.S. and H.S. performed population history reconstructions. J.E., A.H., M.E.S., and G.F.T. performed the species cross. B.F. designed the PCR assays and provided molecular lab support. V.B. performed PCR typing. C.Z., L.M.B., and B.F. produced assemblies and analyzed long-read and chromosome conformation capture (Hi-C) data with support from J.S. F.C.J. performed and analyzed forward-in-time simulations. A.H.H. raised and collected lab populations for sex determination analysis. N.H. performed PCR-typing of lab populations. L.M.B. detected sex-linked inversions in the Lake Victoria radiation. M.K. and Y.F.C. performed haplotagging. I.A. analyzed haplotagging data. W.S., I.A., and H.S. analyzed RNA sequencing data. S.L. and F.Y. performed Fluorescence in situ hybridization (FISH). S.G. produced and analyzed the outgroup variant callset with support from H.S. M.M. produced Hi-C data and the ancestral sequence. D.A.J. contributed the *Diplotaxodon* long-read samples. A.B. provided support for sex chromosome and adaptation related analyses. L.M.B. made the main figures, with input from H.S., V.B., J.C., and I.A. H.S. wrote the manuscript with L.M.B., V.B., J.C., R.D., and further contributions from all authors. All authors read and approved the final manuscript. **Competing interests:** The authors declare that they have no competing interests. **Data and materials availability:** Supporting data are made available in the supplementary materials on an open-access basis for research use only. Accession numbers of raw sequencing data are given in table S1. Accession numbers of other data used are given in the respective materials and methods sections. The main variant callset (VCF) is available as a permanent archive hosted at the University of Cambridge institutional repository (78). Data was collected under appropriate ethical and sampling permits [see materials and methods (38)], and genetic material and sequences are subject to an Access and Benefits Sharing (ABS) agreement with the Government of Malawi. Any person who wishes to use this data for any form of commercial purpose must first enter into a commercial licensing and benefit-sharing arrangement with the Government of Malawi. **License information:** Copyright © 2025 the authors, some rights reserved; exclusive licensee American Association for the Advancement of Science. No claim to original U.S. Government Works. This work is licensed under a Creative Commons Attribution 4.0 International (CC BY 4.0) license, which permits unrestricted use, distribution, and reproduction in any medium, provided the original work is properly cited. To view a copy of this license, visit <https://creativecommons.org/licenses/by/4.0/>. This license does not apply to figures/photos/artwork or other content included in the article that is credited to a third party; obtain authorization from the rights holder before using such material.

SUPPLEMENTARY MATERIALS

science.org/doi/10.1126/science.adr9961

Materials and Methods; Supplementary Text; Figs. S1 to S54; Tables S1 to S31; References (79–178); Data S1 to S8

Submitted 28 July 2024; accepted 9 April 2025

10.1126/science.adr9961